Journal of Catalysis 332 (2015) 62–69

Contents lists available at ScienceDirect

Journal of Catalysis

journal homepage: www.elsevier.com/locate/jcat

Homogeneous and heterogeneous catalysts of organopalladium functionalized-polyhedral oligomeric silsesquioxanes for Suzuki–Miyaura reaction

Vuthichai Ervithayasuporn [a,b], Kwanchanok Kwanplod [a], Jaursup Boonmak [c], Sujittra Youngme [c], Preeyanuch Sangtrirutnugul [a,*]

[a] Department of Chemistry, Center of Excellence for Innovation in Chemistry (PERCH-CIC), Center for Catalysis, and Center for Inorganic and Materials Chemistry, Faculty of Science, Mahidol University, Rama VI Road, Ratchathewi, Bangkok 10400, Thailand
[b] Capability Building Unit for Nanoscience and Nanotechnology, and Center of Intelligent Materials and Systems, Nanotec Center of Excellence, Faculty of Science, Mahidol University, Rama VI Road, Ratchathewi, Bangkok 10400, Thailand
[c] Materials Chemistry Research Center, Department of Chemistry and Center of Excellence for Innovation in Chemistry (PERCH-CIC), Faculty of Science, Khon Kaen University, Khon Kaen 40002, Thailand

ARTICLE INFO

Article history:
Received 8 June 2015
Revised 22 September 2015
Accepted 28 September 2015

Keywords:
Silsesquioxanes
Triazole ligand
Suzuki–Miyaura reactions

ABSTRACT

The mononuclear T_8-Pd and multinuclear T_{10}-Pd catalysts (**3** and **6**) were prepared from a reaction between Pd(COD)Cl_2 (COD = 1,5-cyclooctadiene) and the corresponding octameric T_8 and decameric T_{10} silsesquioxane cages, functionalized with pyridine–triazole ligands. The T_8-Pd complex **3** featuring one Pd(II) center was employed as a homogeneous catalyst for Suzuki–Miyaura cross coupling in a 1:1 EtOH:H_2O solvent. On the other hand, the multinuclear T_{10}-Pd catalyst **6** (*ca.* 4.6 Pd for each T_{10} cage) was obtained as amorphous insoluble materials with exceptionally high molecular Pd loading (1.61 mmol Pd g^{-1}). Under the same catalytic conditions, the homogeneous catalysts **3** exhibited slightly higher activity than the heterogeneous catalyst **6** (initial TOFs = 870 and 690 h^{-1}, respectively). Furthermore, for **6**, 4-(MeO)C_6H_4Br and $PhB(OH)_2$ substrates were catalyzed in the presence of a low catalyst loading of 3.6×10^{-3} mol% Pd under aerobic conditions to afford the coupled product in 91% yield (*i.e.*, turnover number (TON) = 2.5×10^4). The silsesquioxane-supported Pd catalyst **6** was recovered by simple centrifugation and reused for at least five catalytic cycles without a loss in activities.

© 2015 Elsevier Inc. All rights reserved.

1. Introduction

Polyhedral oligomeric silsesquioxanes prepared *via* a hydrolytic-condensation reaction of either alkoxy- or halosilane monomers have been considered as a promising organic–inorganic hybrid precursor. General features of silsesquioxanes include inorganic cage-like silica covalently attached with organic substituents (*e.g.* aryl, vinyl, allyl, and aliphatic-substituted groups) [1–3], which can be designed for subsequent modifications. For example, azido-functionalized polyhedral oligomeric silsesquioxanes are considered reactive materials, which can be further functionalized through "click" reactions [4,5]. These materials containing click linkers have already been used in various applications including electronics [6], polymer nanocomposites [7], bioconjugations [8], and self-assembling dendrimers [9]. However, examples of self-assembled catalytic units on those materials are still rare [10–12]. Recent studies have used polyhedral oligomeric silsesquioxanes as catalyst supports for alkene epoxidation and, in some cases, the resulting catalysts were superior to the homogeneous counterparts in terms of selectivity, efficiency, and reusability [13,14]. In addition, Tang et al. reported that a chiral rhodium catalyst supported on bifunctionalized silsesquioxane-based materials exhibited high performance for asymmetric transfer hydrogenation of aromatic ketones both in enantioselectivity and catalytic activity [15].

Catalytic applications involving 1,2,3-triazole-based ligands have recently been of much interest due to ligand's facile synthesis and convenient substituent modification [16–18]. For example, our group has recently reported the use of Pd(II) complexes featuring the bidentate pyridine–triazole ligands as efficient catalysts for Suzuki–Miyaura cross-coupling reactions [19]. To explore the role of silsesquioxanes as catalyst supports, this work for the first time introduces pyridine–triazole moieties onto the T_n silsesquioxanes. The pyridine–triazole group serves as a bidentate ligand for Pd(II) ions. In particular, the Pd(II) complex supported on the mono pyridine–triazole substituted octameric silsesquioxane was

* Corresponding author.
E-mail address: preeyanuch.san@mahidol.ac.th (P. Sangtrirutnugul).

http://dx.doi.org/10.1016/j.jcat.2015.09.014
0021-9517/© 2015 Elsevier Inc. All rights reserved.

synthesized and investigated as a homogeneous catalyst for Suzuki–Miyaura cross coupling. Similarly, a fully decorated decameric silsesquioxane containing multiple Pd(II) complexes was explored as a heterogeneous catalyst. For Suzuki–Miyaura cross-coupling reactions, the multifunctionalized heterogeneous catalyst promotes not only high catalytic efficiency, but also excellent catalyst recovery while retaining its catalytic activity.

2. Experimental

2.1. Materials

(3-azidopropyl)hepta(*i*-butyl)octasilsesquioxane (**1**) and deca (3-azidopropyl) decasilsesquioxane (**4**) were prepared according to our previous report [4], while Pd(COD)Cl_2 (COD = 1,5-cyclooctadiene) was prepared according to the literature [19]. $CuSO_4$, sodium ascorbate, and 2-ethynylpyridine (purity; 98%), K_2CO_3, and $K_3PO_4{\cdot}H_2O$ were purchased from Sigma Aldrich. Ethyl acetate, dichloromethane and hexane were of commercial grade and distilled prior to use. The pre-coated silica gel 60 F_{254} plates and silica gel (No. 60) used for chromatography were purchased from Merck&Co., Inc.

2.2. Physical measurements and instrumentations

Fourier transform nuclear magnetic resonance spectra of sample solutions were obtained by using Bruker's Ascend 400 high-resolution magnetic resonance spectrometer for ^{1}H (400 MHz), ^{13}C{^{1}H} (100 MHz) and ^{29}Si{^{1}H} (79 MHz) nuclei. The ^{29}Si{^{1}H} CP/MAS NMR spectrum was acquired at 60 MHz frequency with AVANCE 300 MHz Digital NMR Spectrometer (Bruker Biospin; DPX-300). Chemical shifts were reported in δ units (parts per million) relative to tetramethylsilane and residual solvent peaks were used as a reference. High-resolution mass spectra (HRMS) were recorded using a Bruker micro TOF spectrometer in the ESI mode and elemental analyses were performed on a Perkin Elmer 2400 CHN. The ICP-OES and MP-AES spectra were recorded by the inductively coupled plasma optical emission spectrometer, Spectro CIROS^{CCD} and the microwave plasma-atomic emission spectrometer (MP-AES) Systems 4200 MP-AES, respectively. The samples for ICP-OES and MP-AES were prepared as solutions in 2% nitric acid. Powder X-ray diffraction was performed by Bruker D8 Advance with a monochromatic Cu Kα (40 kV, 40 mA) source, step size of 0.010°, and a step time of 3 s/step. Attenuated total reflectance (ATR) Fourier transform infrared spectroscopy (FTIR) measurements were carried out using Bruker Alpha instrument (Bruker Optics GmbH, Ettlingen, Germany) (4000 and 400 cm^{-1}). ATR-FTIR data analysis using OPUS software (Bruker Optic) was applied to pre-process the spectral data. Single-crystal X-ray diffraction of the catalyst **3** ($C_{39}H_{76}Cl_4N_4O_{12}PdSi_8$) was measured on a Bruker D8-Quest PHOTON-100 CMOS detector with graphite-monochromated Mo Kα radiation (λ = 0.71073 Å) using the APEX2 program [20]. Raw data frame integration was performed with SAINT [20]. An empirical absorption correction was applied to the data by the SADABS program [20]. The structure was solved using the direct methods and refined by full-matrix least-squares method on F^2 with anisotropic thermal parameters for all non-hydrogen atoms using the SHELXTL2014 software package [21]. All hydrogen atoms were placed in calculated positions and refined isotropically with a riding model.

2.3. Synthesis of (3-(1H-1,2,3-triazol-4-yl-2-pyridine)propyl)hepta(i-butyl)octasilsesquioxane (2)

A mixture of 2-ethynylpyridine (0.10 mL, 1.02 mmol) and (3-azidopropyl)hepta(*i*-butyl)octasilsesquioxane (**1**) (0.12 g, 0.13 mmol) was dissolved in 5 mL of THF. To this solution mixture were added sodium ascorbate (0.13 g, 0.66 mmol) and $CuSO_4{\cdot}5H_2O$ (8.0 mg, 0.032 mmol) dissolved in deionized water. The solution was then stirred at room temperature for 3 d, after which it was poured into water (30 mL) and extracted with CH_2Cl_2 (3 × 30 mL). The combined organic layers were washed with water and dried with anhydrous Na_2SO_4. Solvent evaporation afforded the crude product, which was further purified by column chromatography with a gradient eluent (10%, 15%, and 20% EtOAc in hexane) to produce the compound **2** as a white solid in 85% yield (0.11 g, 0.11 mmol).

^{1}H NMR (400 MHz, $CDCl_3$, 25 °C): δ 8.58 (d *J* = 4.4 Hz, 1H, Py*H*), 8.21 (s, 1H, N=C*H*), 8.18 (d *J* = 10 Hz, 1H, Py*H*), 7.80 (t *J* = 5.2 Hz, 1H, Py*H*), 7.24 (m, 1H, Py*H*), 4.40 (t *J* = 7.2 Hz, 2H, N—CH_2), 2.05 (quin *J* = 7.7 Hz, 2H, $CH_2CH_2CH_2$), 1.84 (sext *J* = 6.7 Hz, 7H, C*H*(CH_3)$_2$), 0.94 (m, 42H, CH(CH_3)$_2$), 0.65 (overlapped, 2H, CH_2Si), 0.60 (m, 14H, CH_2CH(CH_3)$_2$). ^{13}C{^{1}H} NMR (100 MHz, $CDCl_3$, 25 °C): δ 150.2, 149.0, 147.9, 137.1, 122.8, 121.9, 120.3, 52.7, 25.7, 25.6, 24.1, 23.9, 23.8, 22.4, 22.3, 9.2. ^{29}Si{^{1}H} NMR (79 MHz, $CDCl_3$, 25 °C, TMS): δ −67.51, −67.87, −68.65 (relative intensity ratio = 3:4:1). HRMS (ESI-TOF) calcd. for $C_{38}H_{74}N_4O_{12}Si_8Na$ [M + Na]$^+$: 1025.3355, found 1025.3353. Anal. Calcd. for $C_{38}H_{74}N_4O_{12}Si_8$: C, 45.47; H, 7.43; N, 5.58. Found: C, 45.25; H, 7.82; N, 5.18.

2.4. Synthesis of dichloro-(3-(1H-1,2,3-triazol-4-yl-2-pyridine)propyl) hepta(i-butyl)octa-silsesquioxane palladium(II) complex (3)

A mixture of **2** (0.20 g, 0.20 mmol) and an equimolar of Pd(COD)Cl_2 (0.056 g, 0.20 mmol) in CH_2Cl_2 (8 mL) was stirred at room temperature. After 24 h, glass fiber filtration followed by solvent evaporation gave the crude product as a brown yellow solid. Further recrystallization in CH_2Cl_2 and diethyl ether afforded the catalyst **3** as a dark yellow solid in 55% yield (0.13 g, 0.11 mmol). ^{1}H NMR (400 MHz, $CDCl_3$, 25 °C): δ 8.79 (d *J* = 5.6 Hz, 1H, Py*H*), 8.54 (d *J* = 3.6 Hz, 1H, N=C*H*), 8.04 (s, 1H, Py*H*), 8.03 (s, 1H, Py*H*), 7.29 (t *J* = 4.7 Hz, 1H, Py*H*), 4.59 (t *J* = 7.2 Hz, 2H, N—CH_2), 2.05 (sext *J* = 6.2 Hz, 2H, $CH_2CH_2CH_2$), 1.93 (sext *J* = 6.5 Hz, 7H, C*H*(CH_3)$_2$), 0.94 (d *J* = 6.6 Hz, 42H, CH(CH_3)$_2$), 0.63 (overlapped, 2H, CH_2Si), 0.60 (m, 14H, CH_2CH(CH_3)$_2$). ^{13}C{^{1}H} NMR (100 MHz, $CDCl_3$, 25 °C): δ 149.9, 148.3, 147.6, 140.3, 124.9, 124.6, 122.6, 55.5, 25.7, 23.9, 23.8, 22.4, 22.3, 9.3. ^{29}Si{^{1}H} NMR (79 MHz, $CDCl_3$, 25 °C, TMS): δ −67.45, −67.83, −68.35 (relative intensity ratio 3:4:1). HRMS (ESI-TOF) calcd. for $C_{38}H_{74}N_4O_{12}Si_8PdCl_2Na$ [M + Na]$^+$: 1203.1771, found 1203.1775. Anal. Calcd. for $C_{38}H_{74}N_4O_{12}Si_8PdCl_2$: C, 38.64; H, 6.32; N, 4.74. Found: C, 38.64; H, 6.58; N, 4.84.

2.5. Synthesis of deca(3-(1H-1,2,3-triazol-4-yl-2-pyridine)propyl) decasilsesquioxane (5)

A mixture of 2-ethynylpyridine (0.20 mL, 2.0 mmol) and deca(3-azidopropyl)decasilsesquioxane (**4**) (0.20 g, 0.15 mmol) was dissolved in 5 mL of THF. To this solution mixture was added a catalytic amount of sodium ascorbate (7.4 mg, 0.040 mmol) and $CuSO_4{\cdot}5H_2O$ (4.7 mg, 0.019 mmol) and the solution was stirred at room temperature for 3 d. Then, the reaction mixture was poured into water (30 mL) and extracted with CH_2Cl_2 (3 × 30 mL). The combined organic layers were washed with water and dried with anhydrous Na_2SO_4. Filtration followed by solvent evaporation afforded the crude product, which was purified by column chromatography using 4:1 CH_2Cl_2/MeOH as an eluent. A yellow solid of **5** was obtained in 56% yield (0.20 g, 0.084 mmol). ^{1}H NMR (400 MHz, $CDCl_3$, 25 °C): δ 8.49 (d *J* = 4.0 Hz, 10H, Py*H*), 8.24 (s, 10H, N=C*H*), 8.09 (d *J* = 7.8 Hz, 10H, Py*H*), 7.68 (t *J* = 7.4 Hz, 10H, Py*H*), 7.15 (t *J* = 6.0 Hz, 10H, Py*H*), 4.36 (t *J* = 6.5 Hz, 20H, NCH_2), 1.96 (m, 20H, $CH_2CH_2CH_2$), 0.55 (m, 20H, CH_2Si). ^{13}C{^{1}H} NMR (100 MHz, $CDCl_3$, 25 °C): δ 150.2, 149.2, 148.0, 137.0, 122.8, 122.6, 120.2, 52.4, 24.0, 9.2. ^{29}Si{^{1}H} NMR (79 MHz, $CDCl_3$, 25 °C, TMS): δ

−69.2. HRMS (ESI-TOF) calcd. for $C_{100}H_{111}N_{40}O_{15}Si_{10}Na$ $[M + Na]^+$: 2415.6688, found 2415.6687. Anal. Calcd. for $C_{100}H_{110}N_{40}O_{15}Si_{10}$: C, 50.17; H, 4.67; N, 23.40. Found: C, 50.20; H, 5.03; N, 23.32.

2.6. Synthesis of deca(dichloro-(3-(1H-1,2,3-triazol-4-yl-2-pyridine) propyl))decasilsesquioxane palladium(II) complexes (6)

A mixture of ligand **5** (70 mg, 0.029 mmol) and $Pd(COD)Cl_2$ (83 mg, 0.29 mmol) in CH_2Cl_2 (8 mL) was stirred at room temperature for 3 d. After that, the yellow precipitates were filtered and further washed with 10 mL of CH_2Cl_2 giving an insoluble, dark yellow solid characterized as the complex **6** in 54% yield (50 mg, 0.016 mmol). $^{29}Si\{^1H\}$ CP/MAS NMR (60 MHz, 20 ± 1 °C): δ −70.1. ICP-OES: Pd loading is 1.61 mmol g^{-1} (17.0% by mass). Based on the result from ICP-OES, there is an average of 4.6 Pd ions for each T_{10} silsesquioxane cage. As a result, the average molecular weight of **6** was calculated as a sum of molecular weight of **5** and total weights of 4.6 ($PdCl_2$) fragments.

$$\begin{aligned}\text{Average molecular weight } \mathbf{6} &= \text{molecular weight } \mathbf{5} \\ &\quad + 4.6 \times (\text{molecular weight of } PdCl_2) \\ &= 2394.06 \\ &\quad + 4.6 \times [106.42 + (2 \times 35.45)] \\ &= 3209.73 \text{ g/mol}\end{aligned}$$

2.7. General procedure of Suzuki–Miyaura cross-coupling reaction

RC_6H_4Br (5.0 mmol) and $PhB(OH)_2$ (5.5 mmol) were used as model substrates in the presence of 1 equiv of K_2CO_3 (5.0 mmol) and a 1:1 mixture of EtOH:H_2O (40 mL). Using an appropriated amount of either Pd pre-catalyst **3** or **6**, the reaction mixture was vigorously stirred at 60 °C for the given time, after which 10 mL of H_2O was added and the reaction mixture was extracted with EtOAc (3 × 30 mL). The combined organic layers were dried with anhydrous Na_2SO_4 and filtered. Then, all volatiles were removed *in vacuo*. After that, the crude product was purified by column chromatography on silica gel using EtOAc:hexane (1:9) as an eluent. ^1H NMR spectra of the resulting products can be found in the ESI.

2.8. Hot filtration experiment

To a 1:1 mixture of EtOH:H_2O (8 mL) were added 4-(MeO) C_6H_4Br (1.00 mmol), $PhB(OH)_2$ (1.10 mmol), K_2CO_3 (1.00 mmol), and the catalyst **6** (10 mg, 1.4 mol%). The reaction mixture was stirred at 60 °C for 1 h, after which the hot mixture was quickly filtered. Then, the filtrate was left stirred for additional 3 h. After that, the reaction mixture was worked up using the same procedure as described in Suzuki–Miyaura reactions. Product yields were determined using ^1H NMR spectroscopy with

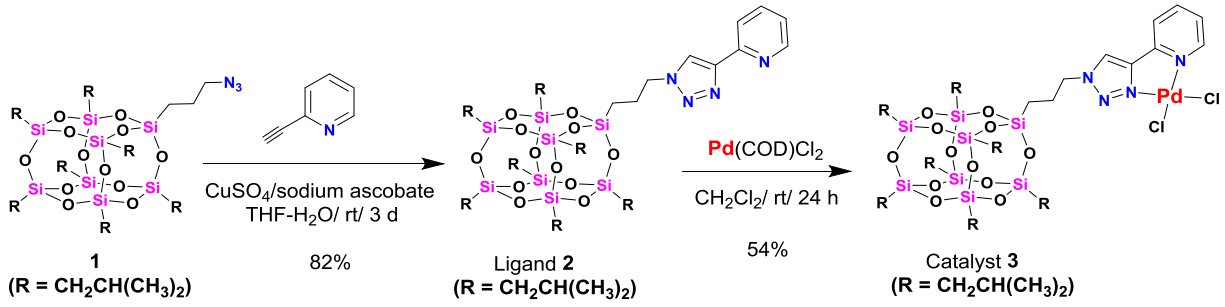

Scheme 1. A synthetic approach for a single catalytic site of polyhedral oligomeric silsesquioxane functionalized with the pyridine–triazole Pd(II) complex (**3**).

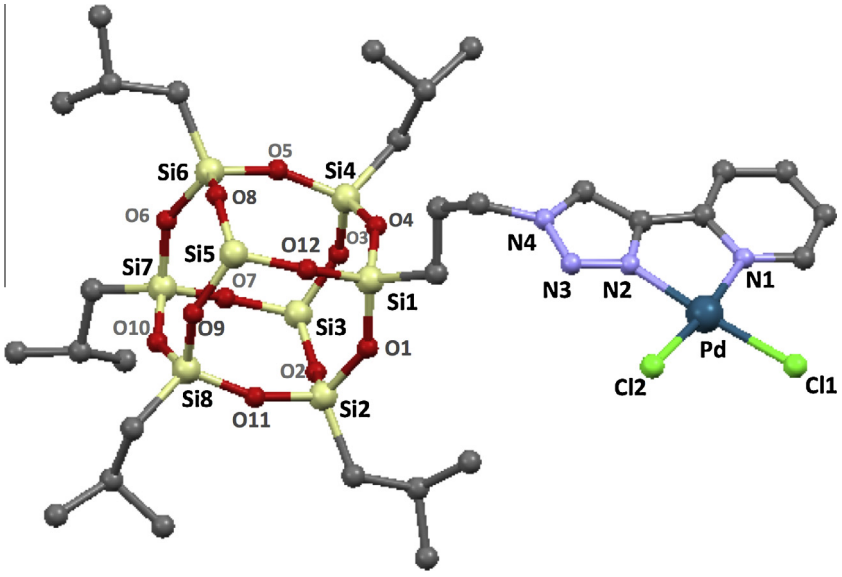

Fig. 1. Ball and stick representation of **3** with a partial atom labeling scheme. A CH_2Cl_2 molecule, two *i*-butyl groups, and hydrogen atoms are omitted for clarity.

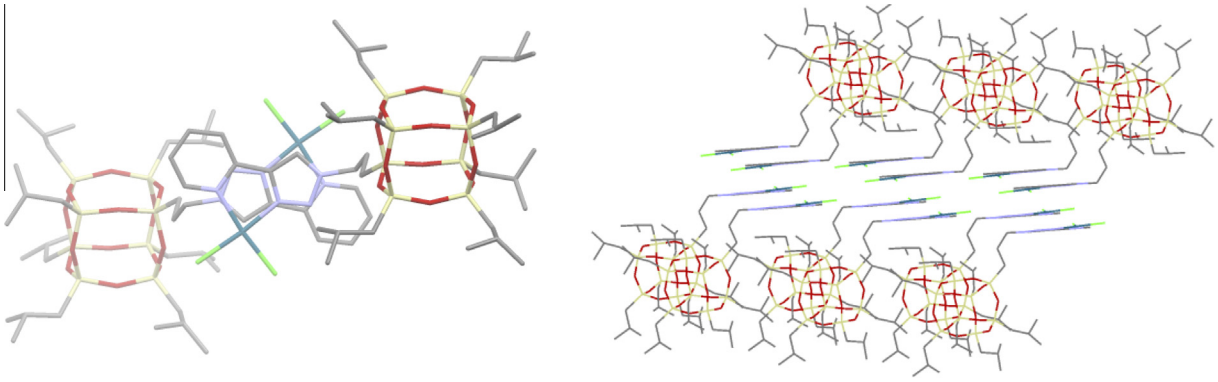

Fig. 2. Stacking diagrams along the direction parallel (left) and perpendicular (right) to the π-stacking direction of **3**.

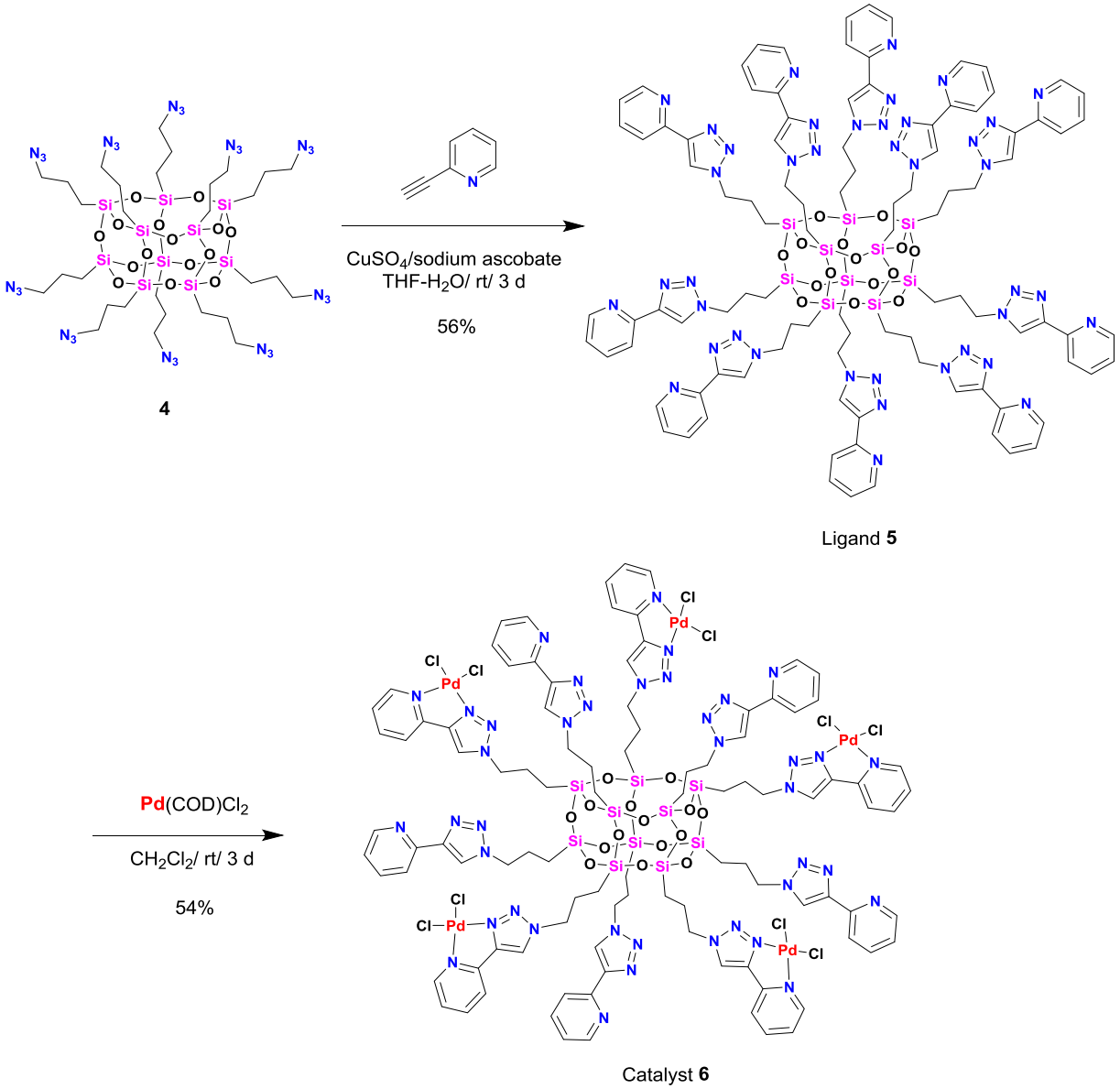

Scheme 2. Synthetic approach for the self-assembled heterogeneous catalyst **6** featuring partial Pd coordination to pyridine–triazole functional groups supported on T_{10} silsesquioxane cage. Based on the ICP-OES result, five Pd ions were depicted.

1,3,5-$(Me)_3C_6H_3$ as an internal standard and the results were shown in Fig. S24, ESI.

3. Results and discussion

3.1. Synthesis and characterizations of silsesquioxanes and catalysts

The starting precursor (3-azidopropyl)hepta(*i*-butyl)octasilsesquioxane (**1**) was prepared according to our previous report [4]. The mono-organoazide group readily reacted with 2-ethynylpyridine under the presence of Cu(I) catalyst to afford the mono-substituted bidentate ligand (3-(1*H*-1,2,3-triazol-4-yl-2-pyridine)propyl)hepta(*i*-butyl)octasilsesquioxane (**2**) in 85% yield, as shown in Scheme 1. A reaction of $Pd(COD)Cl_2$ (COD = 1,5-cyclooctadiene) [22] with an equimolar amount of **2** in CH_2Cl_2 at room temperature resulted in dichloro-(3-(1*H*-1,2,3-triazol-4-yl-2-pyridine)propyl)hepta(*i*-butyl)octasilsesquioxane Pd(II) complex (**3**), crystallized from a CH_2Cl_2:Et_2O solution as a dark yellow crystal, in 54% yield. Due to the presence of hydrophobic *i*-butyl groups on the octameric cage, complex **3** is highly soluble in polar organic solvents (*e.g.* THF, CH_2Cl_2, $CHCl_3$, Et_2O). Upon coordination with Pd, the singlet ^1H NMR resonance ($CDCl_3$) corresponding to the triazole proton (N=C*H*) slightly shifted from δ 8.14 (for **2**) to δ 8.34. The single crystal X-ray analysis of **3** further confirms a distorted square planar structure of Pd with bidentate binding of the pyridine–triazole moiety (Fig. 1). Due to the planar nature of Pd (II) pyridine–triazole metallacycles, complexes **3** are stacked in an anti-parallel manner, through π–π interactions with the centroid–centroid distance of 3.793(3) Å (Fig. 2). Crystallographic data and selected bond lengths and angles are listed in Tables S1 and S2 (ESI).

On the other hand, the fully functionalized azido-substituted polyhedral oligomeric silsesquioxane (T_8, T_{10}, and T_{12}) precursors could be conveniently prepared and isolated from a nucleophilic substitution of NaN_3 on octakis(3-chloropropyl)octasilsesquioxane followed by a simple column chromatography [4]. The cage-rearranged deca(3-azidopropyl)decasilsesquioxane (T_{10}; **4**) obtained as a major product was further reacted with 2-ethynylpyridine *via* a copper-catalyzed azide–alkyne cycloaddition (CuAAC) to give the deca-substituted pyridine–triazole ligand, deca(3-(1*H*-1,2,3-triazol-4-yl-2-pyridine)propyl)decasilsesquioxane (**5**), in 56% yield. A subsequent reaction between **5** and $Pd(COD)Cl_2$ (10 equiv) in CH_2Cl_2 at room temperature afforded the multinuclear Pd(II) complex (**6**), as dark yellow precipitates (Scheme 2). The resulting T_{10}-Pd complex **6** was insoluble in all common solvents investigated including polar organic solvents (*e.g.*, THF, CH_2Cl_2, DMSO, acetone) and polar protic solvents (*e.g.*, MeOH, EtOH, H_2O). The inductively coupled plasma optical emission spectrometry analysis (ICP-OES) of **6** reveals the Pd loading of 1.61 mmol g^{-1} or 17.0 wt%, which is significantly higher than previously reported Pd contents for molecular Pd catalyst on other known solid supports (0.038–0.27 mmol g^{-1}) [23–27]. Based on the amount of Pd, an average of 4.6 Pd(II) ions is coordinated to the pyridine–triazole T_{10} silsesquioxane cage.

To determine the nature of silsesquioxane cage structure, the $^{29}Si\{^1H\}$ MAS NMR spectrum (Fig. 3a) contains a singlet signal at δ −70.1, which is characteristic of T^3 [C—Si(—O—Si)$_3$] [15]. These data suggest that the T_{10}-Pd catalyst **6** possesses a symmetric organosilicate framework. In particular, the decameric silsesquioxane structure was maintained and each silicon atom was covalently bonded to a carbon species. In addition, XPS analysis of **6** confirms the presence of Pd(II) ions based on the existence of two binding energy peaks at 338.3 and 343.5 eV assignable to $3d_{5/2}$ and $3d_{3/2}$, respectively (Fig. 3b) [28]. Thus, we suggest that catalyst **6** exists as a combination of multinuclear complexes containing different Pd complex units, firmly held by the bidentate pyridine–triazole ligands. As a result, **6** is expected to be a stable Pd (II)-containing heterogeneous catalyst. In addition, the crystallinity of these silsesquioxane-based compounds was evaluated using powder X-ray diffraction (XRD) techniques. The diffractograms of the T_8 ligand **2** and the T_8-Pd catalyst **3** contain diffracted peaks, indicating crystalline structures. This is due to the highly symmetrical structure of the T_8 silsesquioxane cage (O_h), which allows favorable molecular packing (Fig. 4a and b). On contrary, we did

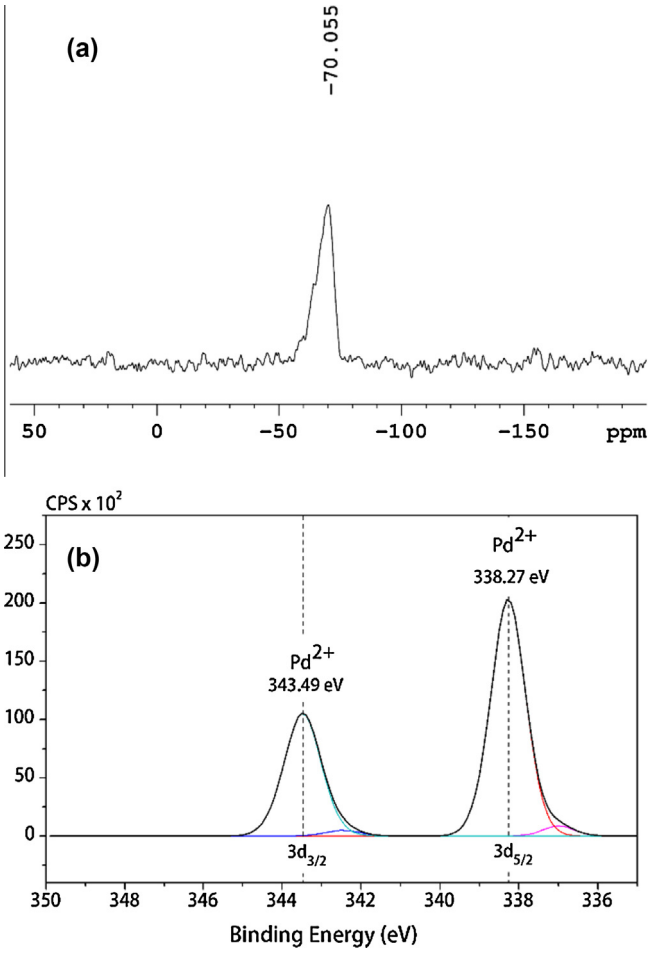

Fig. 3. (a) $^{29}Si\{^1H\}$ MAS NMR and (b) XPS spectra of the T_{10}-Pd catalyst **6**.

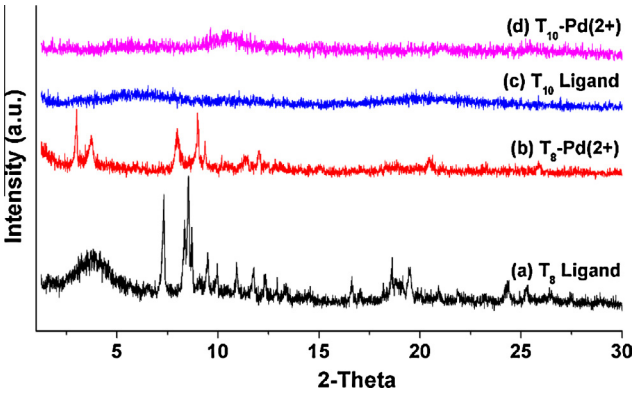

Fig. 4. XRD spectra of (a) T_8 ligand **2**, (b) T_8-Pd catalyst **3**, (c) T_{10} ligand **5**, and (d) T_{10}-Pd catalyst **6**.

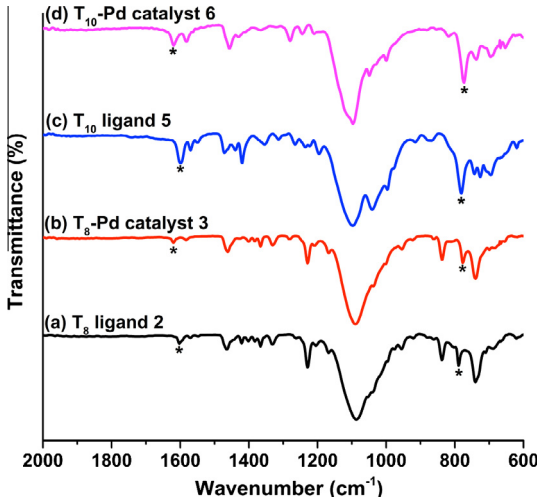

Fig. 5. FT-IR spectra of (a) T_8 ligand **2**, (b) T_8-Pd catalyst **3**, (c) T_{10} ligand **5**, and (d) T_{10}-Pd catalyst **6**.

not observe any XRD signals for the amorphous T_{10} ligand **5** and T_{10}-Pd **6** (Fig. 4c and d). This finding is consistent with our previous work, which showed that the crystallinity of an aromatic functionalized T_{10} silsesquioxane cage (D_{5h}) was significantly diminished, compared to its T_8 analog (O_h) as a result of lower symmetry of an inorganic silicate core of the T_{10} cage [29]. For **5**, the liquid state and the absence of signals in powder XRD suggest disordered arrangements of T_{10} molecules. Interestingly, upon an addition of Pd(II), the physical state immediately changes from liquid to a dark yellow solid. On a basis of a high number of rigid planar Pd(II) pyridine–triazole metallacycles present for each T_{10} cage, it is reasonable to suspect that a certain degree of Pd(II)-induced, self-assembled π-stacking interactions, as shown in the crystal packing of the Pd complex **3** (Fig. 2), occurs causing the insolubility of the catalyst **6**. However, no XRD peak is observed in the diffractogram, possibly due to an incomplete Pd complexation and low symmetry of T_{10} cages (Fig. 4d).

To further probe π-stacking interactions, infrared spectroscopy was applied to the pyridine–triazole T_8 and T_{10} ligands and their corresponding Pd(II) complexes T_8-Pd (**3**) and T_{10}-Pd (**6**) in the solid state. Fig. 5(a–d) shows that the aromatic C—C stretching bands are blue-shifted after Pd coordination from 1603 cm^{-1} to 1620 cm^{-1} (for **2** and **3**) and from 1599 cm^{-1} to 1619 cm^{-1} (for **5** and **6**). In addition, IR bands assignable to C—H vibrations out of the plane to the aromatic ring are red-shifted from 789 cm^{-1} to 777 cm^{-1} (for **2** and **3**) and from 781 cm^{-1} to 773 cm^{-1} (for **5** and **6**). These results indicate stronger π–π stacking interactions of the Pd catalysts **3** and **6**, compared to the free ligands, which consequently lead to more rigid aromatic rings and the weakening of the aromatic C—H bonds [30,31].

3.2. Catalytic studies

The catalytic activities of **3** (T_8-Pd) and **6** (T_{10}-Pd) toward Suzuki–Miyaura cross-coupling were evaluated using 4-(MeO)C_6H_4Br and $PhB(OH)_2$ as model substrates with a K_2CO_3 base. To optimize the reaction conditions, an effect of different bases on catalytic activities was investigated, in which K_2CO_3 was shown to afford the highest product yields (Table S3, ESI). Under the same catalytic conditions, the catalyst **3** was completely soluble in the reaction medium (*e.g.*, 1:1 EtOH:H_2O), while **6** appeared as a brown suspension. Under the same reaction conditions, both the homogeneous catalyst **3** and the heterogeneous catalyst **6** with similar Pd contents gave almost quantitative coupling yields of 98% and 91%

Table 1
Suzuki–Miyaura cross-couplings of ArBr and $PhB(OH)_2$ catalyzed by **3** and **6**.

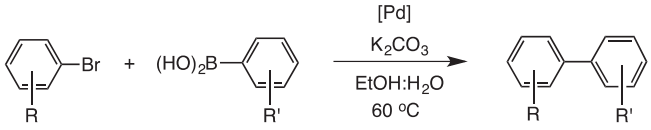

Entry	[Pd] Catalyst	mol% Pd[a]	R	R′	Time (h)	Yield (%)[b]	**TON**[c]
1[d]	**3**	3.0×10^{-2}	4-OMe	H	12	98(100)[e]	3.3×10^3
2[f]	**6**	2.9×10^{-2}	4-OMe	H	12	91(93)[e]	3.1×10^3
3[g]	**6**	7.2×10^{-3}	4-OMe	H	24	97	1.3×10^4
4[h]	**6**	3.6×10^{-3}	4-OMe	H	24	91	2.5×10^4
5[i]	**6**	0.15	4-COMe	H	12	92	613
6[j]	**6**	1.4	4-OMe	H	4	93	66
7[j]	**6**	1.4	3-OMe	H	4	87	62
8[j]	**6**	1.4	2-OMe	H	4	65	46
9[j]	**6**	1.4	4-CHO	H	12	89	64
10[j]	**6**	1.4	4-Me	H	12	83	59
11[j]	**6**	1.4	4-OMe	4-OMe	4	70	50
12[j]	**6**	1.4	4-OMe	3-OMe	4	65	46
13[j]	**6**	1.4	4-OMe	2-OMe	4	15	11
14[j]	**6**	1.4	4-OMe	4-COMe	4	46	33

[a] mol% Pd for catalyst **6** = [(mass of T_{10}-Pd catalyst **6**) × 4.6 × 100]/[(MW of T_{10}-Pd catalyst **6**) × mol ArBr].
[b] Isolated yields.
[c] TON = (% yield)/(mol% Pd).
[d] Reaction conditions: 4-RC_6H_4Br (5.0 mmol), $PhB(OH)_2$ (5.5 mmol), K_2CO_3 (5.0 mmol), 1.9 mg **3**, EtOH:H_2O (1:1, 20 mL) at 60 °C.
[e] ^1H NMR yield (using 1,3,5-$(Me)_3C_6H_3$ as an internal standard),
[f] 4-RC_6H_4Br (5.0 mmol), $PhB(OH)_2$ (5.5 mmol) and K_2CO_3 (5.0 mmol), 1.0 mg **6** in EtOH:H_2O (1:1, 40 mL).
[g] 4-RC_6H_4Br (20 mmol), $PhB(OH)_2$ (22 mmol) and K_2CO_3 (20 mmol), 1.0 mg **6** in EtOH:H_2O (1:1, 160 mL).
[h] 4-RC_6H_4Br (40 mmol), $PhB(OH)_2$ (44 mmol) and K_2CO_3 (40 mmol), 1.0 mg **6** in EtOH:H_2O (1:1, 160 mL).
[i] 4-RC_6H_4Br (0.5 mmol), $PhB(OH)_2$ (0.55 mmol) and $K_3PO_4{\cdot}H_2O$ (0.6 mmol), 1.1 mg **6** in toluene (2.0 mL) at 100 °C.
[j] 4-RC_6H_4Br (0.5 mmol), $ArB(OH)_2$ (0.55 mmol) and K_2CO_3 (0.5 mmol), 5.0 mg **6** in EtOH:H_2O (1:1, 4 mL).

Table 2
Recycling experiments of the catalyst **6**[a].

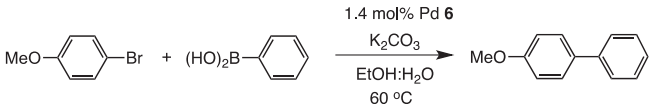

Run	1	2	3	4	5
Yield (%)[b]	92	97	97	89	91

[a] Conditions: 4-(MeO)C_6H_4Br (1.0 mmol), $PhB(OH)_2$ (1.1 mmol), catalyst **6** (10 mg, 1.4 mol% Pd) and K_2CO_3 (1.0 mmol) in EtOH:H_2O (1:1, 8 mL), 8 h.
[b] Isolated yields *via* column chromatography.

after 12 h (entries 1 and 2, Table 1). In addition, a plot of product percentage yields at various reaction times reveals slightly faster coupling reactions in the presence of the homogeneous catalyst **3** compared to **6** (Fig. S17, ESI). In particular, after 2 h, initial TOF values of **3** and **6** are 870 and 690 h^{-1}, respectively. It should be noted that previous studies have often reported a significant decrease in catalytic activities with supported catalysts compared to the homogeneous analogs [32–34]. However, based on the obtained initial TOF values of **3** and **6**, we suggest that the heterogeneous catalyst **6** represents an amorphous materials with non close-packed or disorder arrangements allowing good exposure of the Pd active sites. Since ICP-OES of the heterogeneous catalyst **6** revealed an average of 4.6 Pd ions for each T_{10} molecule, the turnover number (TON) was calculated based on mol% of Pd. The C—C cross couplings catalyzed by the catalyst **6** with the Pd content as low as 3.6×10^{-3} mol% resulted in the high product yield of 91% after 24 h at 60 °C, giving the maximum TON of *ca.* 25,000 (entry 4). In addition, under the same conditions (*i.e.*, with $K_3PO_4 \cdot H_2O$ base at 100 °C in toluene, 12 h), the catalyst **6** produced a higher product yield (92%; entry 5 Table 1) than those reported with the commercial heterogeneous Pd EnCat TPP30 and Pd EnCat NP30 catalysts (80% and 70%, respectively) [35].

To evaluate the generality of the heterogeneous catalyst **6** toward other substrates, various aryl bromides and arylboronic acids were used (entries 6–14, Table 1). For the methoxy-substituted aryl bromides, under the same reaction conditions, the lowest product yield (65%) was obtained from the most sterically hindered substrate 2-(MeO)C_6H_4Br (entries 6–8). Furthermore, electronic properties of aryl bromide substrates did not have a significant effect on the product yields (entries 6, 9, and 10). On the other hand, cross couplings between 4-(MeO)C_6H_4Br and different aryl substituted $ArB(OH)_2$ generally resulted in lower product yields than that of $PhB(OH)_2$ (entries 6, 11–14). Based on the electronic effect, 4-(MeO)$C_6H_4B(OH)_2$ containing the electron-donating methoxy substituent gave a higher product yield (70%; entry 11) than that obtained from the electron-withdrawing substrate 4-(MeCO)$C_6H_4B(OH)_2$ (46%; entry 14). For a steric reason, the presence of a methoxy group at the *ortho* position of $ArB(OH)_2$ also significantly reduced the coupling yield (15%; entry 13). In addition, the more challenging ArCl substrate 4-ClC_6H_4CHO was also investigated but, unfortunately, no C—C cross-coupling product was observed even in the presence of 3.0 mol% of **6** at 100 °C after 1 d. The recyclability of **6** was also determined using 4-(MeO)C_6H_4Br and $PhB(OH)_2$ substrates. With 1.4 mol% Pd, high isolated product yields (89–97%) were obtained through five successive reaction cycles without a loss in catalytic activities (Table 2). After each catalytic run, the T_{10}-Pd catalyst **6** could be easily separated from the reaction mixtures *via* centrifugation. Hot filtration tests were carried out to determine the heterogeneity nature of **6** [36]. Based on ^1H NMR spectra, we did not observe any increase in the product yields after catalyst removal at 1 h (Fig. S24, ESI). Furthermore, microwave plasma-atomic emission spectroscopy (MP-AES) reveals that the reaction filtrate obtained after completion of the Suzuki–Miyaura reaction (entry 6, Table 1) contains <0.10 ppm of Pd species, confirming minimal Pd leaching from **6** during catalysis.

4. Conclusions

The homogeneous catalyst T_8-Pd (**3**) featuring a monomeric Pd complex is prepared through ligand exchange between $Pd(COD)Cl_2$ and the pyridine–triazole substituted T_8 cage at room temperature. Meanwhile, the insoluble materials or heterogeneous catalyst T_{10}-Pd (**6**) with an amorphous character containing exceptionally high Pd content (*i.e.*, 1.6 mmol Pd g^{-1} or *ca.* 4.6 Pd ions for each decameric cage) is also generated under similar conditions. For the Suzuki–Miyaura reactions, the catalyst **3** is slightly more active than **6**, as evidenced by initial TOFs of 870 h^{-1} (for **3**) and 690 h^{-1} (for **6**). These results suggest effective Pd-substrate interactions in **6**, despite its heterogeneous nature. Furthermore, remarkable robustness and convenient catalyst separation of **6** allow for efficient catalyst reuse. In conclusion, we demonstrate that polyhedral oligomeric silsesquioxanes serve as a promising ligand scaffold, which affords catalysts with desirable features including high catalytic activity, stability, and good recyclability.

Acknowledgments

This research is financially supported by two Grants from the Thailand Research Fund: TRG5780232 (for Ervithayasuporn, V.) and RSA5780058 (for Sangtrirutnugul, P.). The authors also gratefully acknowledge Center of Excellence for Innovation in Chemistry (PERCH-CIC), Faculty of Science, Mahidol University and Mahidol University under the National Research Universities Initiative, the Nanotechnology Center (NANOTEC), NSTDA, Ministry of Science and Technology, Thailand, through its program of Center of Excellence Network.

Appendix A. Supplementary material

Supplementary data associated with this article can be found, in the online version, at http://dx.doi.org/10.1016/j.jcat.2015.09.014.

References

[1] D.B. Cordes, P.D. Lickiss, F. Rataboul, Chem. Rev. 110 (2010) 2081.
[2] V. Ervithayasuporn, S. Chimjarn, Inorg. Chem. 52 (2013) 13108.
[3] R.H. Baney, M. Itoh, A. Sakakibara, T. Suzuki, Chem. Rev. 95 (1995) 1409.
[4] V. Ervithayasuporn, X. Wang, Y. Kawakami, Chem. Commun. (2009) 5130.
[5] S. Fabritz, D. Heyl, V. Bagutski, M. Empting, E. Rikowski, H. Frauendorf, I. Balog, W.-D. Fessner, J.J. Schneider, O. Avrutina, H. Kolmar, Org. Biomol. Chem. 8 (2010) 2212.
[6] V. Ervithayasuporn, J. Abe, X. Wang, T. Matsushima, H. Murata, Y. Kawakami, Tetrahedron 66 (2010) 9348.
[7] J. Choi, S.G. Kim, R.M. Laine, Macromolecules 37 (2004) 99.
[8] S. Fabritz, S. Hörner, O. Avrutina, H. Kolmar, Org. Biomol. Chem. 11 (2013) 2224.
[9] X. Wang, V. Ervithayasuporn, Y. Zhang, Y. Kawakami, Chem. Commun. 47 (2011) 1282.
[10] P. Guillo, M.E. Fasulo, M.I. Lipschutz, T.D. Tilley, Dalton Trans. 2013 (1991) 42.
[11] M. Ventura, M.E.G. Mosquera, T. Cuenca, B. Royo, G. Jiménez, Inorg. Chem. 51 (2012) 6345.
[12] R. Duchateau, Chem. Rev. 102 (2002) 3525.
[13] Y. Leng, J. Zhao, P. Jiang, J. Wang, RSC Adv. 5 (2015) 17709.
[14] Y. Leng, J. Liu, C. Zhang, P. Jiang, Catal. Sci. Technol. 4 (2014) 997.
[15] S. Tang, R. Jin, H. Zhang, H. Yao, J. Zhuang, G. Liu, H. Li, Chem. Commun. 48 (2012) 6286.
[16] M. Meldal, C.W. Tornøe, Chem. Rev. 108 (2008) 2952.
[17] V.V. Rostovtsev, L.G. Green, V.V. Fokin, K.B. Sharpless, Angew. Chem., Int. Ed. 41 (2002) 2596.
[18] C.W. Tornøe, C. Christensen, M.J. Meldal, J. Org. Chem. 67 (2002) 3057.

[19] S. Jindabot, K. Teerachanan, P. Thongkam, S. Kiatisevi, T. Khamnaen, P. Phiriyawirut, S. Charoenchaidet, T. Sooksimuang, P. Kongsaeree, P. Sangtrirutnugul, J. Organomet. Chem. 750 (2014) 35.
[20] Bruker, Bruker AXS Inc., Madison, WI, USA, 2007.
[21] G.M. Sheldrick, Acta Cryst. A64 (2008) 112.
[22] D. Drew, J.R. Doyle, A.G. Shaver, in: Inorg. Synth, John Wiley & Sons Inc., 2007, p. 346.
[23] M. Ghotbinejad, A.R. Khosropour, I. Mahammadpoor-Baltork, M. Moghadam, S. Tangestaninejad, V.J. Mirkhani, Mol. Catal. A: Chem. 385 (2014) 78.
[24] B. Karimi, F. Mansouri, H. Vali, Green Chem. 16 (2014) 2587.
[25] S.M. Sarkar, M.L. Rahman, M.M. Yusoff, RSC Adv. 5 (2015) 1295.
[26] C. Sarmah, D. Sahu, P. Das, Catal. Today 198 (2012) 197.
[27] P. Sharma, A.P. Singh, RSC Adv. 4 (2014) 43070.
[28] J.P. Mathew, M. Srinivasan, Eur. Polym. J. 31 (1995) 835.
[29] S. Chimjarn, R. Kunthom, P. Chancharone, R. Sodkhomkhum, P. Sangtrirutnugul, V. Ervithayasuporn, Dalton Trans. 44 (2015) 916.
[30] D. Zhang, L. Fu, L. Liao, N. Liu, B. Dai, C. Zhang, Nano Res. 5 (2012) 875.
[31] Y. Zhang, S. Yuan, W. Zhou, J. Xu, Y. Li, J. Nanosci. Nanotechnol. 7 (2007) 1.
[32] A. Corma, D. Das, H. García, A. Leyva, J. Catal. 229 (2005) 322.
[33] S. MacQuarrie, B. Nohair, J.H. Horton, S. Kaliaguine, C.M. Crudden, J. Phys. Chem. C 114 (2010) 57.
[34] H. Yang, X. Han, Z. Ma, R. Wang, J. Liu, X. Ji, Green Chem. 12 (2010) 441.
[35] C. Diebold, J.M. Becht, J. Lu, P.H. Toy, C.L. Drian, Eur. J. Org. Chem. (2012) 893.
[36] H.E.B. Lempers, R.A. Sheldon, J. Catal. 175 (1998) 62.